



Evaluation and docking of indole sulfonamide as a potent inhibitor of α -glucosidase enzyme in streptozotocin –induced diabetic albino wistar rats

Muhammad Taha^{a,*}, Syahrul Imran^b, Mohammed Salahuddin^a, Naveed Iqbal^c, Fazal Rahim^d, Nizam Uddin^e, Adeeb Shehzad^a, Rai Khalid Farooq^f, Munther Alomari^g, Khalid Mohammed Khan^h

^a Department of Clinical Pharmacy Research, Institute for Research and Medical Consultations (IRMC), Imam Abdulrahman Bin Faisal University, P.O. Box 31441, Dammam, Saudi Arabia

^b Atta-ur-Rahman Institute for Natural Product Discovery, Universiti Teknologi MARA (UiTM), Puncak Alam Campus, 42300 Bandar Puncak Alam, Selangor, Malaysia

^c Department of Chemistry University of Poonch, Rawalakot, AJK, Pakistan

^d Department of Chemistry, Hazara University, Mansehra 21300, Khyber Pakhtunkhwa, Pakistan

^e Department of Chemistry, University of Karachi, Karachi 75270, Pakistan

^f Department of Neuroscience Research, Institute for Research and Medical Consultations (IRMC), Imam Abdulrahman Bin Faisal University, P.O. Box 1982, Dammam 31441, Saudi Arabia

^g Department of Stem Cell Biology, Institute for Research and Medical Consultations (IRMC), Imam Abdulrahman Bin Faisal University, P.O. Box 1982, Dammam 31441, Saudi Arabia

^h H. E. J. Research Institute of Chemistry, International Center for Chemical and Biological Sciences, University of Karachi, Karachi 75270, Pakistan

ARTICLE INFO

Keywords:

α -Glucosidase inhibitors
Indole analogs
SAR
Molecular docking
In vivo

ABSTRACT

We have synthesized new hybrid class of indole bearing sulfonamide scaffolds (1–17) as α -glucosidase inhibitors. All scaffolds were found to be active except scaffold 17 and exhibited IC_{50} values ranging from 1.60 to 51.20 μ M in comparison with standard acarbose (IC_{50} = 42.45 μ M). Among the synthesized hybrid class scaffolds 16 was the most potent analogue with IC_{50} value 1.60 μ M, showing many folds better potency as compared to standard acarbose. Whereas, synthesized scaffolds 1–15 showed good α -glucosidase inhibitory potential. Based on α -glucosidase inhibitory effect, Scaffold 16 was chosen due to highest activity *in vitro* for further evaluation of antidiabetic activity in Streptozotocin induced diabetic rats. The Scaffold 16 exhibited significant antidiabetic activity. All analogues were characterized through 1H , ^{13}C NMR and HR MS. Structure-activity relationship of synthesized analogues was established and confirmed through molecular docking study.

1. Introduction

To maintain healthy activities of body the α -glucosidase enzyme catalyzes carbohydrates. Some serious problems to human health are associated with higher activity of α -glucosidase that leads to increase in blood glucose level [1–4]. In type-2 diabetes various α -glucosidase inhibitors are used to maintain the sugar level of blood [5,6]. So far various clinically used α -glucosidase inhibitors are acarbose, miglitol and voglibose etc [7,8]. Inhibitors are usually administered orally that leads to carbohydrates digestion and absorption delay, resulting to maintain the glucose level [9–11]. Medicinal chemists focused on the synthesis of new α -glucosidase inhibitors as these inhibitors had various side effects. Pharmaceutical community takes keen interest in the

synthesis of α -glucosidase inhibitors that possess catalytic potency to decrease blood glucose level that in turn result to decrease glucose absorption [12–14]. α -Glucosidase inhibitors do not show life threatening condition and its overdose does not show weight gain or hyperglycemic effects in body [15]. Beside diabetes, α -glucosidase inhibitors showed meaningful application in obesity and in other medical therapeutics [16] and in case of HIV infections showed remarkable proliferation that result to block viral infections [17,18]. Due to these aspects, we have synthesized hybrid indole bearing sulfonamide as new class of inhibitors.

Indoles are a heterocyclic analogue that occurs in various natural products as secondary metabolites such as alkaloids, marine secondary metabolites and fungal secondary metabolites etc [19,20]. A lot of

* Corresponding author.

E-mail address: mtaha@iau.edu.sa (M. Taha).

<https://doi.org/10.1016/j.bioorg.2021.104808>

Received 19 January 2021; Received in revised form 25 February 2021; Accepted 2 March 2021

Available online 10 March 2021

0045-2068/© 2021 Elsevier Inc. All rights reserved.

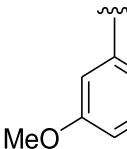
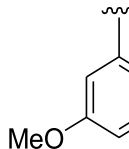
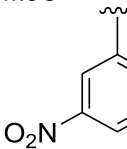
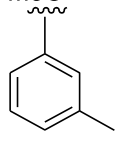
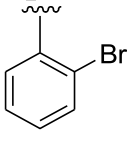
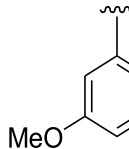
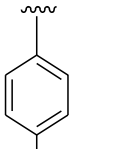
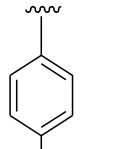
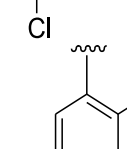
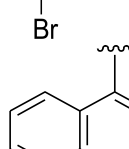
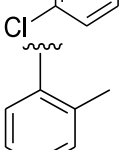
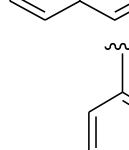
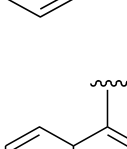
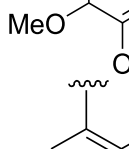
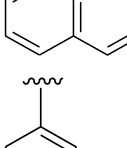
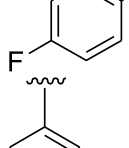
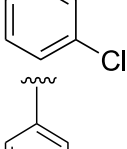
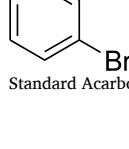
indole scaffolds showed its consideration in medicinal chemistry as well as in organic synthesis. Indole and its scaffolds showed broad range of biological potential such as antibacterial [21], anticancer [22], anti-malarial [23], anti-ulcerative [24], anti-leishmanial [25], anti-platelet [26], anti-rheumatoid [27], antioxidant [28], anti-viral [19], anti-HIV [29], thymidine phosphorylase, as well as inhibitors of β -glucuronidase [30,31].

In the synthesis of various groups of drugs sulfonamides moiety act as a basic skeleton that are also names as sulpha drugs or sulfa drugs [32,33]. To produce new effect/action in the previously synthesized

biologically active scaffold the sulfonamide functional group showed its great potency e.g, Alzheimer's disease associated butyrylcholinesterase (BChE) enzyme potent inhibitors have been synthesized from its previously marketed lead scaffold of sulfonamide that exhibited excellent potency at low concentration [34,35]. Similarly, sulfonamide scaffolds from the decades have been extensively used against certain disease that are multifarious than bacterial infections like AD, diabetes [36], psychosis [37], central nervous system (CNS) disorders [38], tumors [39] and different cancer treatments [40].

Our research group had previously synthesized different

Table 1
Synthesized hybrid indole bearing sulfonamide scaffolds (1–17).

S. No	R	IC ₅₀ (μ M)	S. No	R	IC ₅₀ (μ M)
1		7.30 \pm 0.20	10		21.30 \pm 0.30
2		4.70 \pm 0.20	11		28.50 \pm 0.20
3		51.20 \pm 1.10	12		31.30 \pm 0.50
4		8.20 \pm 0.50	13		35.80 \pm 0.60
5		8.40 \pm 0.010	14		41.20 \pm 0.20
6		14.30 \pm 0.20	15		41.90 \pm 0.80
7		15.20 \pm 0.30	16		1.60 \pm 0.010
8		16.70 \pm 0.30	17		N.A.
9		21.10 \pm 0.40			42.45 \pm 1.05
				Standard Acarbose	

heterocycles as well as their hybrid analogues and evaluated against different biological potential [41]. Keeping in view, the biological importance of indole as well as sulfonamide scaffold we plan to design, synthesis of new hybrid class of indole bearing sulfonamide scaffolds that might show promising results upon comparison with individual scaffolds.

1.1. Result and discussion

1.1.1. Chemistry

The indole-based sulfonamide scaffolds (1–17) were synthesized by treating 2-(1H-indol-3-yl) ethanamine with various aryl sulfonyl chloride in the presence of pyridine. The reaction completion was confirmed by monitoring TLC. All synthesized compounds were recrystallized in methanol. The purity of compounds was confirmed by proton NMR as well as HR MS. All compounds were fully characterized different spectroscopy method (Table 1) Scheme 1.

1.1.2. α -Glucosidase inhibition

The synthesized hybrid indole bearing sulfonamide scaffolds (1–17) were for their α -glucosidase inhibitory potential [42–44]. All scaffolds were found active except scaffold 17. Different inhibitory potential was exhibited by scaffolds 1–15 with IC_{50} value ranging between 1.60 ± 0.010 – 51.20 ± 1.10 μ M upon comparison with standard acarbose (42.45 ± 1.05 μ M). Scaffold 16 exhibited IC_{50} value 1.60 ± 0.010 many folds better than standard acarbose and is the most potent scaffold among the synthesized derivatives. Similarly scaffold 1, 2, 4 and 5 exhibited IC_{50} values ranging 4.70–8.40 μ M showing 10 to 5 folds more potency than standard.

The methyl substituted scaffolds 6, 9, 11 are the *ortho*, *para* and *meta* substituted scaffolds that showed IC_{50} value 14.30 ± 0.20 , 21.10 ± 0.40 and 28.50 ± 0.20 respectively. From IC_{50} values of enzyme inhibition pattern it was confirm that *ortho* substituted > *para* substituted > *meta* substituted scaffold.

Scaffold 4, 5, which are mono and dichloro substituted derivatives exhibited IC_{50} value 8.20 ± 0.50 and 8.40 ± 0.010 , respectively. It was observed that addition of chloro as substituent might be responsible for slight decrease in potency.

The bromo substituted scaffolds 3, 13 are the *ortho*, *para* substituted scaffolds that showed IC_{50} value 51.20 ± 1.10 , 35.80 ± 0.60 respectively, while scaffold 17 *meta* substituted was found inactive. From IC_{50} values of the scaffold it was confirmed that *ortho* substituted scaffold showed greater potential as compared to *para* substituted and *meta* substituted scaffold was the inactive as compared to *ortho* and *para* substituted scaffold.

It was confirmed that type, number/s and position of substituent/s might play a role in slight increase or decrease in α -glucosidase inhibitory potency.

1.1.3. Results of animals study

1.1.3.1. Hypoglycemic effect of Scaffold 16. Based on the excellent results of *in vitro* and molecular docking study showed by Scaffold 16,

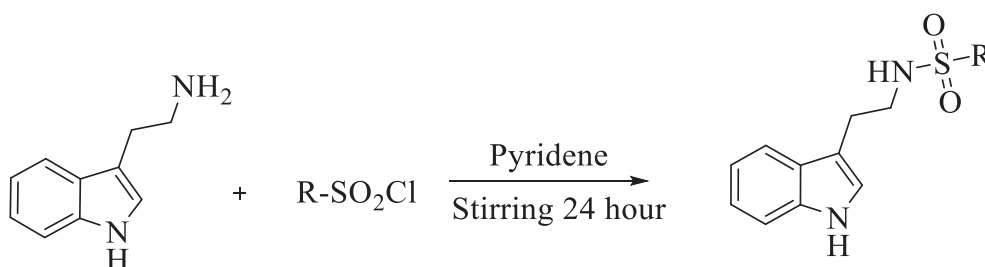
antidiabetic activity in rats was designed and carried out. Acute toxicity study was carried out at dose of 1000 mg/kg body weight and no toxicity was found. Hence, three scalar doses 10, 25, & 50 mg/kg body weight were selected for preliminary screening of Scaffold 16 for hypoglycemic effect, and similar approach has been reported earlier [49]. The compound was administered orally, and blood glucose level measured up to 6 h duration and the compound was found to be effective till 4 h duration and reduced the blood glucose level significantly ($***p < 0.001$), as compared to the diabetic control group. Scaffold 16 significantly decreases the blood glucose level at 2 h (17%) and 4 h (24%) at a dose of 50 mg/kg, as compared to the values of 30 min and diabetic control group. Whereas, at 25 mg/kg dose, scaffold 16 reduces 17% of blood glucose level, as compared to values at 1 h and diabetic control group (Fig. 1). No significant changes were observed in the blood glucose level of animals treated with Scaffold 16- 10 mg/kg body weight. After 4 h of duration, the blood glucose levels in scaffold 16 treated groups started inclined towards the higher values.

1.1.3.2. Effects of scaffold 16 on fasting blood glucose and body weight.

To find out the long-term beneficial effects of Scaffold 16 on fasting blood glucose levels and body weights of animals, two scalar doses were selected based on results of acute hypoglycemic effects (Fig. 1). These doses of the compound were administered at a dose of 25 and 50 mg/kg body orally for 28 days. On every 7th day interval, fasting blood glucose and body weights were measured. Standard drug, Glibenclamide was given at a dose of 5 mg/kg body weight for the same duration. It has been found that the fasting blood glucose level of Scaffold 16 treated group decreases significantly ($***p < 0.001$), as compared to the values of 1st day and diabetic control group. The fasting blood glucose level of the group treated with scaffold 16 at dose 25 mg/kg body was reduced to 317.83 mg/dl on day 28 from the initial level of 440 mg/dl on day 1 (decrease of 28%). Higher reduction of fasting blood glucose level was observed with the dose of 50 mg/kg, which reduced the initial blood glucose level of 511 mg/dl to 241 mg/dl on 28th day (reduction of 53%) (Fig. 2). Significant effect ($***p < 0.001$) was observed in the group treated with standard drug Glibenclamide, which reduced 41% of fasting blood glucose level on day 28, as compared to day 1.

Every week, body weight of all groups of animals were measured in order to know the effect of Scaffold 16 treatment, and was compared to normal, diabetic control and standard group. It has been found that there is significant ($***p < 0.001$) improvement on day 28 in the body weight of the animals treated with Scaffold 16 (25 and 50 mg/kg body weight), as compared to body weight of animals on day 14 (Fig. 3). Initial treatment of Scaffold 16 for 14 days failed to show any protection on loss of body weight. Body weight of animals treated with Glibenclamide was improved significantly and was more stable throughout study, as compared to the diabetic control and Scaffold 16 treated group.

1.1.3.3. Effect of Scaffold-16 on oral glucose tolerance test (OGTT). On 28th day of the study, OGTT was carried out in fasted diabetic rats. The animals were observed for 120 min duration, after administration of Scaffold 16 at doses of 25 and 50 mg/kg body weight. There was significant increase in the blood glucose levels of all the groups at 0.5 h of



Scheme 1. The indole-based sulfonamide scaffolds (1–17) were synthesized.

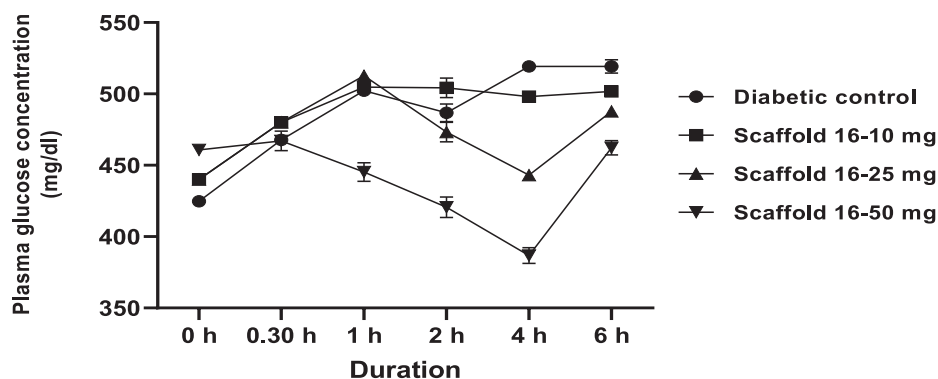


Fig. 1. Hypoglycemic Effects of Scaffold-16. Values are expressed as the mean \pm standard error of the mean ($n = 6$). *** $P < 0.001$ Compared to Diabetic control and 1 h (25 mg /kg); *** $P < 0.001$ Compared to Diabetic control and 0.5 h (50 mg /kg).

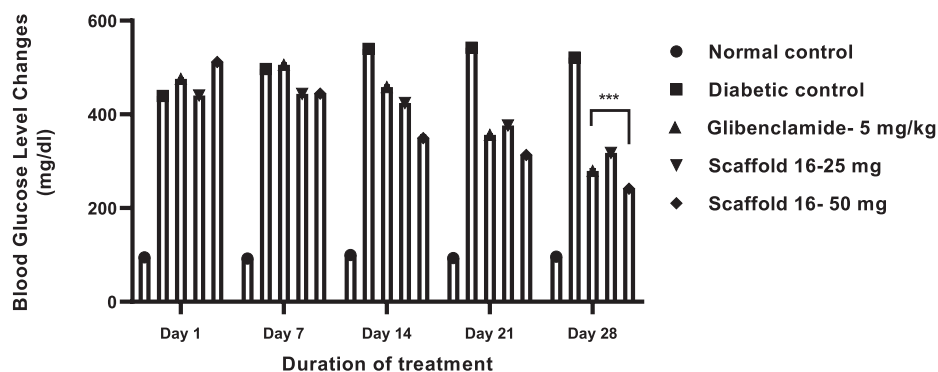


Fig. 2. Effect of Scaffold-16 on Fasting Blood Glucose Levels Values are expressed as the mean \pm standard error of the mean ($n = 6$). *** $P < 0.001$ Compared to Diabetic control and Day 1.

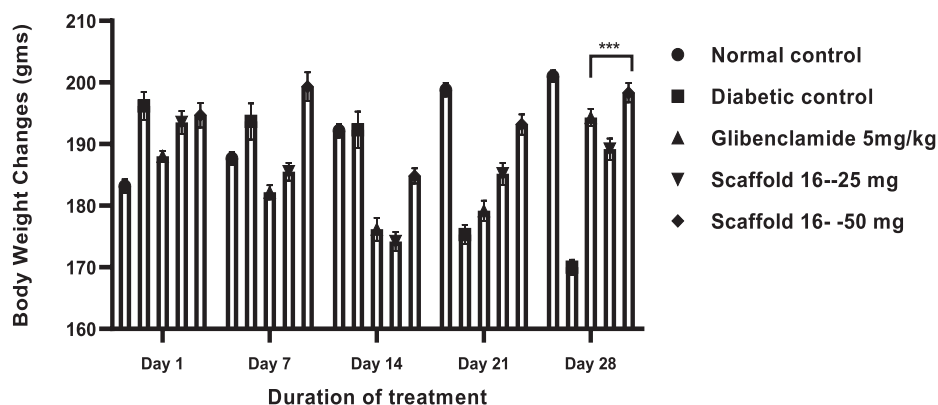


Fig. 3. Effect of Scaffold-16 on Body weight of Animals. Values are expressed as the mean \pm standard error of the mean ($n = 6$). *** $P < 0.001$ Compared to Diabetic control and Day 14.

OGTT, as compared to the level of 0 h. The glucose response failed in diabetic control group of animals, whereas the animals treated with scaffold 16 showed significant tolerance after 1 h of duration. After 2 h of administration Scaffold 16, the blood glucose levels were reduced to below initial blood glucose levels (Fig. 4).

The changes in the blood glucose level was used to calculated area under the curve. As compared to level at 0.5 h, Scaffold 16 at a dose of 25 mg/kg body weight reduced the areas under the curve (AUC) for glucose by 36.90% and 43.30% at 50 mg/kg, whereas, Glibenclamide reduces 20.62%, after 2 h of administration (Fig. 5). Area under curve for Scaffold 16 at 25 and 50 mg/kg body weight was 55,765 and 53,408, as compared to the 63,677 of Diabetic control group. Area under curve was calculated by using Gaphpad Prism 8.0.1.

1.1.4. Docking study

The docking results the most active compound 16 displayed interaction involving extended aromatic ring bearing chloro at *ortho* position. The chloro substituent at *ortho* position interacts with the backbone of Arg312 through hydrophobic alkyl interaction at 3.91 Å. Besides that, the backbone of Arg312 also played an important role in making sure that the extended aromatic ring is stable in the active site by interacting with the π -orbital of the aromatic ring through a π -alkyl interaction at 4.32 Å. On the other hand, some hydrogen bonds were observed as well. It was observed that one of the oxygens of sulfonamide moiety forms a conventional hydrogen bonding with the backbone (HD) of Asn241 at 1.88 Å. While another hydrogen bonding was observed between hydrogen of amino group with the backbone (Ne2) of His279 at 2.06 Å.

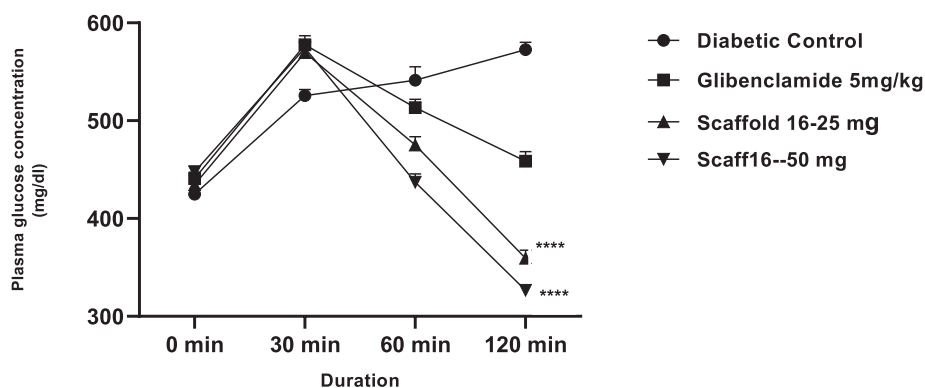


Fig. 4. Oral Glucose Tolerance Test. Values are expressed as the mean \pm standard error of the mean ($n = 6$). *** $P < 0.001$ Compared to Diabetic control and 0.5 h.

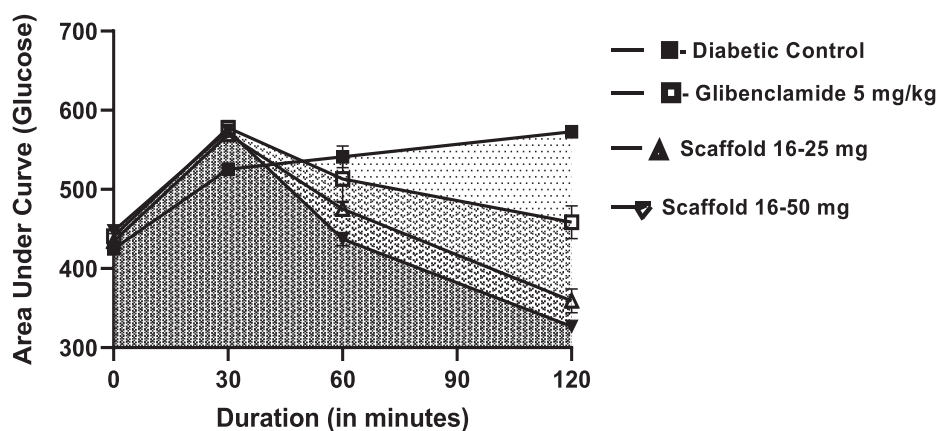


Fig. 5. Area Under Curve Values are expressed as the mean \pm standard error of the mean ($n = 6$). *** $P < 0.001$ Compared to Diabetic control and 0.5 h.

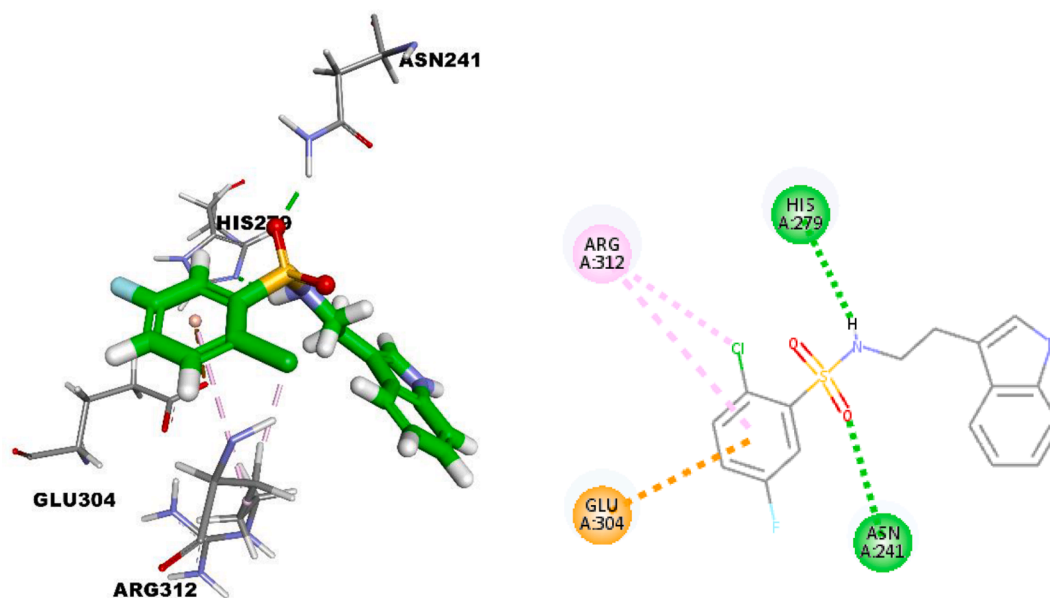


Fig. 6. Interaction of most active compound 16 with residues in the active site.

(Fig. 6).

In the case of the second most active compound 2, it was observed that the extended aromatic ring can interact with various residues with the active site. The results showed that one of the oxygen atoms of the nitro group is forming a conventional hydrogen bonding with the hydrogen (He1) on the backbone of His279 at 2.99 Å. On the other hand,

one of the nitrogen (Ne2) on imidazole ring of His279 further stabilizes the interaction by acting as a hydrogen bond acceptor and interacts with hydrogen (H36) on amino group of the sulfonamide moiety at a distance of 2.25 Å. It was also observed that oxygen (Oe2) on Glu304 can form two electrostatic interactions with nitrogen (N23) of nitro substituent and π -orbital of the extended aromatic ring. Glu304 forms an

electrostatic attractive charge interaction with nitro substituent at 4.20 Å while on the extended aromatic ring, Glu304 forms an electrostatic π -anion interaction at 3.60 Å. It was observed that one of the oxygens of sulfonamide moiety forms a conventional hydrogen bonding with the backbone (HD22) of Asn241 at 2.09 Å (Fig. 7).

For the third most active compounds **1**, hydrogen (H39) on methoxy substituent interacts with Thr307 backbone oxygen at 2.81 Å through carbon hydrogen bond (Fig. 8). Oxygen (O23) of methoxy substituent interacts with the backbone of Thr301 (HG1) through a conventional hydrogen bond at 2.05 Å. Extended aromatic ring is stabilized by electrostatic π -anion interaction with backbone of Glu304 (O ϵ 1) at 3.44 Å and also a hydrophobic π -alkyl interaction with Arg312 at a distance of 4.15 Å. On the other hand, some hydrogen bonds were observed as well. It was observed that both oxygens of sulfonamide moiety can form conventional hydrogen bonds. One of the oxygens of sulfonamide moiety forms a hydrogen bonding with Asn241 (HD22) at 2.13 Å while the other oxygen atom forms a hydrogen bonding with His239 (HE1) at 2.96 Å. While another hydrogen bonding was observed between hydrogen of amino group with the backbone (NE2) of His279 at 2.10 Å. Phe157 is potentially involved in two hydrophobic π - π stakeing interactions with indole moiety at 4.51 and 5.17 Å, which may have resulted in better complex stability.

2. Experimental

2.1. Synthesis procedure for hybrid indole bearing sulfonamide

The synthesis of indole-based sulfonamide was carried out by reacting 2-(1H-indol-3-yl) ethanamine (1 mmol) with various aryl sulfonyl chloride (1.1 mmol each) in the presence of pyridine (10 mL). The reaction was remained on stirring overnight. The confirmation of completion of reaction was monitored by TLC. After completion of reaction the mixture was poured in dilute solution of HCl to kill pyridine. The ppt formed was filtered and washed with cold water. The crude products were recrystallized in methanol to afford pure indole-based sulfonamide scaffolds (**1–17**) in good yields. The purity of compounds was confirmed by proton NMR as well as HR MS (Fig. 9) general figure of compounds (**1–17**).

2.1.1. *N*-(2-(1H-indol-3-yl)ethyl)-2-fluoro-4-methoxybenzenesulfonamide (**1**)

^1H NMR (400 MHz DMSO- d_6): δ ^1H NMR (400 MHz DMSO- d_6): δ 12.70 (s, 1H, NH), 10.92 (s, 1H, NH), 7.87 (t, J = 6.7 Hz, 1H), 7.58 (d, J = 6.9 Hz, 1H), 7.34 (d, J = 6.5 Hz, 1H), 7.14 (d, J = 2.2 Hz, 1H) 7.06 (t,

J = 6.4 Hz, 1H), 7.02 (t, J = 6.1 Hz, 1H), 6.88–6.83 (m, 2H), 3.94 (t, J = 6.5 Hz, 2H), 3.03 (t, J = 6.5 Hz, 2H); ^{13}C NMR (100 MHz, DMSO- d_6): δ 162.1, 136.1, 132.6 (d, J = 182, C-F), 129.3, 127.0, 122.8, 121.4, 119.5, 118.5, 118.0, 112.5, 111.0, 110.0, 102.5, 55.5 (OCH $_3$), 43.5, 27.6; HREI-MS: m/z 348.0935; [($M+1$) $^+$] Calcd for C $_{17}$ H $_{17}$ FN $_2$ O $_3$ S 348.0943.

2.1.2. *N*-(2-(1H-indol-3-yl)ethyl)-2-chloro-5-nitrobenzenesulfonamide (**2**)

^1H NMR (400 MHz DMSO- d_6): δ ^1H NMR (400 MHz DMSO- d_6): δ 14.13 (s, 1H, NH), 10.92 (s, 1H, NH), 8.33 (d, J = 2.1 Hz, 1H), 8.02 (d, J = 6.0 Hz, 1H), 7.62 (d, J = 6.7 Hz, 1H), 7.36 (d, J = 6.4 Hz, 1H), 7.19 (d, J = 2.4 Hz, 1H) 7.09 (t, J = 6.3 Hz, 1H), 6.99 (t, J = 6.1 Hz, 1H), 6.57 (d, J = 7.3, Hz, 1H), 3.95 (t, J = 6.2 Hz, 2H), 3.15 (t, J = 6.2 Hz, 2H); ^{13}C NMR (100 MHz, DMSO- d_6): δ 152.0, 145.0, 136.1, 132.6, 129.1, 127.0, 124.4, 122.8, 122.0, 121.4, 119.5, 118.5, 112.5, 111.0, 43.5, 27.6; HREI-MS: m/z 379.0381; [($M+1$) $^+$] Calcd for C $_{16}$ H $_{14}$ ClN $_3$ O $_4$ S 379.0393.

2.1.3. *N*-(2-(1H-indol-3-yl)ethyl)-2-bromobenzenesulfonamide (**3**)

^1H NMR (400 MHz DMSO- d_6): δ ^1H NMR (400 MHz DMSO- d_6): δ 11.56 (s, 1H, NH), 10.53 (s, 1H, NH), 7.88 (t, J = 6.7 Hz, 1H), 7.65–7.62 (m, 2H), 7.57 (d, J = 6.9 Hz, 1H), 7.36–7.32 (m, 2H), 7.19 (d, J = 2.4 Hz, 1H) 7.13 (t, J = 6.2 Hz, 1H), 7.07 (t, J = 6.2 Hz, 1H), 3.93 (t, J = 6.3 Hz, 2H), 3.14 (t, J = 6.3 Hz, 2H); ^{13}C NMR (100 MHz, DMSO- d_6): δ 142.2, 136.1, 134.4, 130.2, 129.2, 127.8, 127.0, 122.8, 121.4, 120.3, 119.5, 118.5, 112.5, 111.0, 43.5, 27.6; HREI-MS: m/z 378.0023; [($M+1$) $^+$] Calcd for C $_{16}$ H $_{15}$ BrN $_2$ O $_2$ S 378.0037].

2.1.4. *N*-(2-(1H-indol-3-yl)ethyl)-4-chlorobenzenesulfonamide (**4**)

^1H NMR (400 MHz DMSO- d_6): δ 12.09 (s, 1H, NH), 11.12 (s, 1H, NH), 7.90 (d, J = 6.7 Hz, 2H), 7.54 (d, J = 6.9 Hz, 1H), 7.33 (d, J = 6.4 Hz, 2H), 7.15–7.05 (m, 3H), 3.90 (t, J = 6.2 Hz, 2H), 3.11 (t, J = 6.2 Hz, 2H); ^{13}C NMR (100 MHz, DMSO- d_6): δ 143.0, 137.0, 136.1, 129.0, 129.0, 128.5, 128.5, 127.0, 122.8, 121.4, 119.5, 118.5, 112.5, 111.0, 43.5, 27.6; HREI-MS: m/z 334.0530; [($M+1$) $^+$] Calcd for C $_{16}$ H $_{15}$ ClN $_2$ O $_2$ S 334.0522.

2.1.5. *N*-(2-(1H-indol-3-yl)ethyl)-2,5-dichlorobenzenesulfonamide (**5**)

^1H NMR (400 MHz DMSO- d_6): δ 13.81 (s, 1H, NH), 10.8 (s, 1H, NH), 7.57 (d, J = 6.7 Hz, 1H), 7.47 (t, J = 2.4 Hz, 2H), 7.34–7.31 (m, 2H), 7.14 (t, J = 2.4 Hz, 2H), 7.07 (t, J = 6.3 Hz, 1H), 6.98 (t, J = 6.1 Hz, 1H), 6.88 (t, J = 7.5 Hz, 2H), 3.90 (t, J = 6.2 Hz, 2H), 3.11 (t, J = 6.2 Hz, 2H); ^{13}C NMR (100 MHz, DMSO- d_6): δ 138.1, 137.5, 136.1, 132.6, 130.5, 130.0, 127.5, 127.0, 122.8, 121.4, 119.5, 118.5, 112.5, 111.0, 43.5, 27.6; HREI-MS: m/z 368.0530; [($M+1$) $^+$] Calcd for C $_{16}$ H $_{14}$ Cl $_2$ N $_2$ O $_2$ S 368.0153.

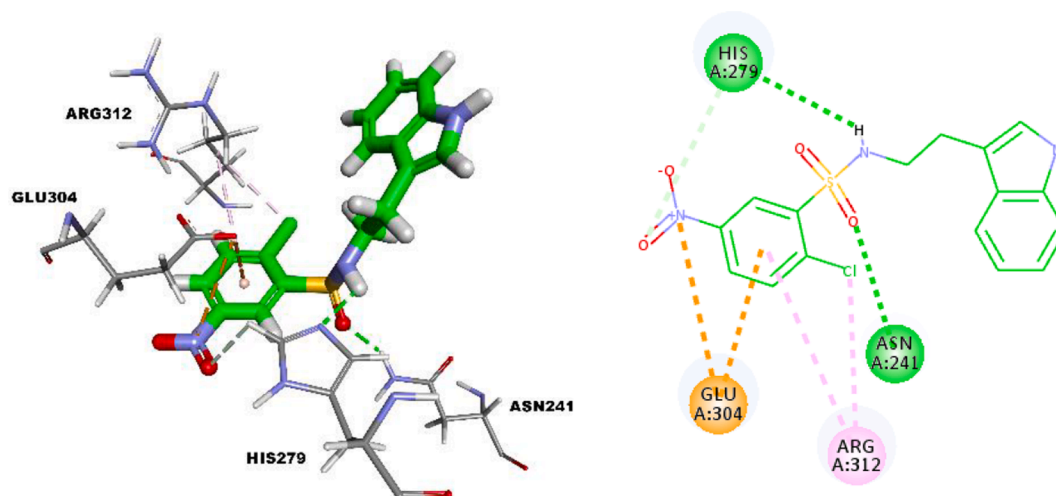


Fig. 7. Interaction of second most active compound **2** with residues in the active site.

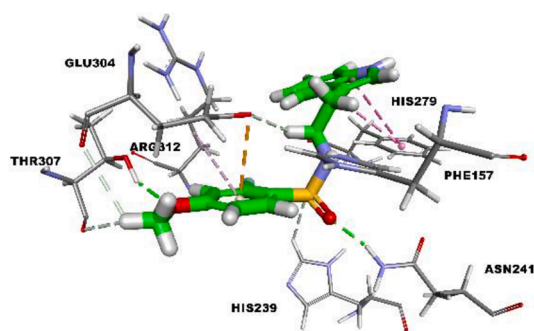


Fig. 8. Interaction of third most active compound 1 with residues in the active site.

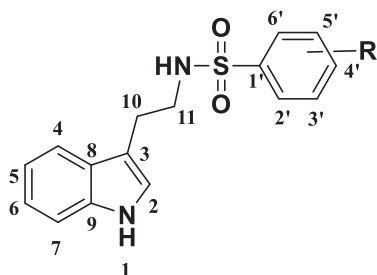


Fig. 9. General Figure of indole-based sulfonamide analogs (1–17).

2.1.6. *N*-(2-(1*H*-indol-3-yl)ethyl)-2-methylbenzenesulfonamide (6)

^1H NMR (400 MHz DMSO- d_6): δ 13.38 (s, 1H, NH), 10.52 (s, 1H, NH), 7.93 (t, J = 6.4 Hz, 1H), 7.69–7.66 (m, 2H), 7.60 (d, J = 6.4 Hz, 1H), 7.39–7.35 (m, 2H), 7.22 (d, J = 2.2 Hz, 1H), 7.17 (t, J = 6.7 Hz, 1H), 7.10 (t, J = 6.4 Hz, 1H), 3.96 (t, J = 6.7 Hz, 2H), 3.12 (t, J = 6.7 Hz, 2H), 2.10 (s, 3H, CH₃); ^{13}C NMR (100 MHz, DMSO- d_6): δ 138.5, 136.1, 135.6, 131.1, 131.5, 129.5, 127.0, 122.8, 121.4, 120.3, 119.5, 118.5, 112.5, 111.0, 43.5, 27.6, 21.5 (CH₃); HREI-MS: m/z 314.1073; [(M+1)⁺ Calcd for C₁₇H₁₈N₂O₂S 314.1089].

2.1.7. *N*-(2-(1*H*-indol-3-yl)ethyl)-2-hydroxynaphthalene-1-sulfonamide (7)

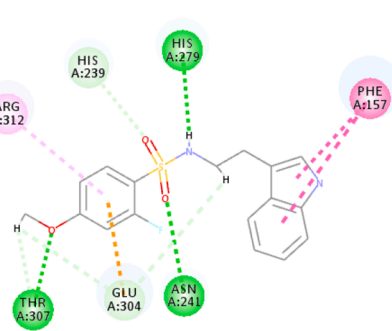
^1H NMR (400 MHz DMSO- d_6): δ 14.04 (s, 1H, NH), 10.93 (s, 1H, NH), 9.03 (s, 1H, OH), 7.95 (t, J = 6.7 Hz, 1H), 7.62–7.58 (m, 2H), 7.54 (d, J = 6.3 Hz, 1H), 7.33–7.29 (m, 2H), 7.19 (d, J = 2.4 Hz, 1H), 7.14 (t, J = 6.3 Hz, 1H), 7.07 (t, J = 6.2 Hz, 1H), 7.00 (t, J = 6.6 Hz, 1H), 6.66 (d, J = 6.3 Hz, 1H), 3.93 (t, J = 6.7 Hz, 2H), 3.08 (t, J = 6.7 Hz, 2H); ^{13}C NMR (100 MHz, DMSO- d_6): δ 148.1, 137.5, 136.1, 127.5, 127.0, 126.6, 126.3, 126.0, 124.0, 122.8, 122.5, 122.1, 121.4, 119.5, 119.1, 118.5, 112.5, 111.0, 43.5, 27.6; HREI-MS: m/z 366.1029; [(M+1)⁺ Calcd for C₂₀H₁₈N₂O₃S 366.1038].

2.1.8. *N*-(2-(1*H*-indol-3-yl)ethyl)-3-chlorobenzenesulfonamide (8)

^1H NMR (400 MHz DMSO- d_6): δ 12.13 (s, 1H, NH), 10.83 (s, 1H, NH), 7.64 (t, J = 6.6 Hz, 2H), 7.53 (d, J = 6.4 Hz, 1H), 7.42 (d, J = 6.7 Hz, 1H), 7.19 (t, J = 6.2 Hz, 2H), 7.14 (t, J = 6.1 Hz, 1H), 7.02 (t, J = 6.2 Hz, 1H), 7.00 (t, J = 6.6 Hz, 1H), 6.76 (t, J = 6.2 Hz, 1H), 3.88 (t, J = 6.4 Hz, 2H), 3.06 (t, J = 6.4 Hz, 2H); ^{13}C NMR (100 MHz, DMSO- d_6): δ 141.0, 136.1, 134.1, 132.5, 130.3, 127.0, 126.1, 125.1, 122.8, 121.4, 119.5, 118.5, 112.5, 111.0, 43.5, 27.6; HREI-MS: m/z 334.0532; [(M+1)⁺ Calcd for C₁₆H₁₅ClN₂O₂S 334.0542].

2.1.9. *N*-(2-(1*H*-indol-3-yl)ethyl)-4-methylbenzenesulfonamide (9)

^1H NMR (400 MHz DMSO- d_6): δ 12.64 (s, 1H, NH), 10.92 (s, 1H, NH), 7.89 (t, J = 6.3 Hz, 1H), 7.72 (t, J = 6.1 Hz, 2H), 7.55 (d, J = 6.7 Hz, 1H), 7.36–7.30 (m, 2H), 7.22 (t, J = 6.3 Hz, 1H), 7.06–7.02 (m, 2H), 3.91 (t, J = 6.2 Hz, 2H), 3.09 (t, J = 6.2 Hz, 2H); ^{13}C NMR (100 MHz, DMSO- d_6): δ 137.5, 137.0, 136.1, 129.0, 129.0, 128.1, 128.1, 127.0, 122.8, 121.4,



119.5, 118.5, 112.5, 111.0, 43.5, 27.6, 21.4 (CH₃); HREI-MS: m/z 314.1073; [(M+1)⁺ Calcd for C₁₇H₁₈N₂O₂S 314.1089].

2.1.10. *N*-(2-(1*H*-indol-3-yl)ethyl)-3-iodo-5-methoxybenzenesulfonamide (10)

^1H NMR (400 MHz DMSO- d_6): δ 12.21 (s, 1H, NH), 10.88 (s, 1H, NH), 7.76 (t, J = 6.3 Hz, 1H), 7.71 (t, J = 6.2 Hz, 1H), 7.47–7.42 (m, 2H), 7.24 (t, J = 6.1 Hz, 2H), 7.08 (t, J = 2.4 Hz, 1H), 7.01 (d, J = 7.2 Hz, 1H), 3.85 (t, J = 6.4 Hz, 5H), 3.07 (t, J = 6.0 Hz, 2H); ^{13}C NMR (100 MHz, DMSO- d_6): δ 162.0, 142.0, 136.1, 127.0, 126.1, 124.5, 122.8, 121.4, 119.5, 118.5, 112.5, 111.0, 110.0, 95.4, 55.5 (OCH₃), 43.5, 27.6; HREI-MS: m/z 455.9989; [(M+1)⁺ Calcd for C₁₇H₁₇IN₂O₃S 456.0004].

2.1.11. *N*-(2-(1*H*-indol-3-yl)ethyl)-3-methylbenzenesulfonamide (11)

^1H NMR (400 MHz DMSO- d_6): δ 11.76 (s, 1H, NH), 10.76 (s, 1H, NH), 7.60 (t, J = 6.1 Hz, 2H), 7.49 (d, J = 6.2 Hz, 1H), 7.39 (d, J = 6.3 Hz, 1H), 7.15 (t, J = 7.2 Hz, 1H), 7.20 (t, J = 6.4 Hz, 1H), 7.04 (t, J = 6.3 Hz, 1H), 6.74 (t, J = 6.2 Hz, 2H), 3.85 (t, J = 4.6 Hz, 5H), 3.09 (t, J = 6.3 Hz, 2H), 2.14 (s, 3H, CH₃); ^{13}C NMR (100 MHz, DMSO- d_6): δ 139.5, 138.4, 136.1, 132.5, 128.5, 127.0, 126.5, 124.1, 122.8, 121.4, 119.5, 118.5, 112.5, 111.0, 43.5, 27.6, 21.5 (CH₃); HREI-MS: m/z 314.1073; [(M+1)⁺ Calcd for C₁₇H₁₈N₂O₂S 314.1089].

2.1.12. *N*-(2-(1*H*-indol-3-yl)ethyl)-3,5-dimethoxybenzenesulfonamide (12)

^1H NMR (400 MHz DMSO- d_6): δ 11.98 (s, 1H, NH), 10.73 (s, 1H, NH), 7.75 (dd, J = 2.3, 2.4 Hz, 1H), 7.73 (d, J = 2.3 Hz, 1H), 7.44 (d, J = 6.1 Hz, 1H), 7.42 (t, J = 6.2 Hz, 1H), 7.39 (t, J = 6.1 Hz, 1H), 7.09 (t, J = 6.6 Hz, 1H), 6.98 (t, J = 6.2 Hz, 2H), 6.82 (t, J = 2.0 Hz, 1H), 3.95 (t, J = 6.4 Hz, 2H), 3.82 (s, 6H, 2xCH₃), 3.06 (t, J = 6.4 Hz, 2H); ^{13}C NMR (100 MHz, DMSO- d_6): δ 161.2, 161.2, 142.0, 136.1, 127.0, 122.8, 121.4, 119.5, 118.5, 112.5, 111.0, 103.5, 103.0, 103.0, 55.5 (OCH₃), 55.5 (OCH₃), 43.5, 27.6; HREI-MS: m/z 360.1131; [(M+1)⁺ Calcd for C₁₈H₂₀N₂O₄S 360.1143].

2.1.13. *N*-(2-(1*H*-indol-3-yl)ethyl)-4-bromobenzenesulfonamide (13)

^1H NMR (400 MHz DMSO- d_6): δ 11.22 (s, 1H, NH), 9.56 (s, 1H, NH), 7.73 (t, J = 6.5 Hz, 1H), 7.49 (d, J = 7.2 Hz, 2H), 7.43 (d, J = 6.1 Hz, 1H), 7.25 (d, J = 7.2 Hz, 2H), 7.01–6.96 (m, 2H), 3.93 (t, J = 6.6 Hz, 2H), 3.13 (t, J = 6.6 Hz, 2H); ^{13}C NMR (100 MHz, DMSO- d_6): δ 143.1, 136.1, 131.3, 131.3, 129.0, 129.0, 127.0, 126.0, 122.8, 121.4, 119.5, 118.5, 112.5, 111.0, 43.5, 27.6; HREI-MS: m/z 378.0023; [(M+1)⁺ Calcd for C₁₆H₁₅BrN₂O₂S 378.0037].

2.1.14. *N*-(2-(1*H*-indol-3-yl)ethyl)naphthalene-1-sulfonamide (14)

^1H NMR (400 MHz DMSO- d_6): δ 10.81 (s, 1H, NH), 9.04 (s, 1H, NH), 8.87 (d, J = 6.7 Hz, 1H), 7.72 (t, J = 6.1 Hz, 2H), 7.55 (d, J = 6.7 Hz, 1H), 7.36–7.30 (m, 2H), 7.22 (t, J = 6.3 Hz, 1H), 7.06–7.02 (m, 2H), 3.91 (t, J = 6.2 Hz, 2H), 3.09 (t, J = 6.2 Hz, 2H); ^{13}C NMR (100 MHz, DMSO- d_6): δ 137.4, 136.5, 136.1, 134.3, 129.1, 128.0, 128.0, 127.0, 126.3, 125.5, 123.5, 123.5, 122.8, 121.4, 119.5, 118.5, 112.5, 111.0,

43.5, 27.6; HREI-MS: m/z 350.1076; $[(M+1)^+]$ Calcd for $C_{20}H_{18}N_2O_2S$ 350.1089].

2.1.15. *N*-(2-(1*H*-indol-3-yl)ethyl)-2-bromo-4,5-dimethoxybenzenesulfonamide (15)

1H NMR (400 MHz DMSO- d_6): δ 12.64 (s, 1H, NH), 10.92 (s, 1H, NH), 8.89 (t, J = 6.3 Hz, 1H), 8.01–7.97 (m, 3H), 7.68–7.64 (m, 3H), 7.52 (t, J = 6.7 Hz, 1H), 7.32 (d, J = 6.4 Hz, 1H), 7.19 (d, J = 6.3 Hz, 1H), 7.04–7.01 (m, 3H), 3.91 (t, J = 6.2 Hz, 2H), 3.09 (t, J = 6.2 Hz, 2H); ^{13}C NMR (100 MHz, DMSO- d_6): δ 153.1, 149.3, 136.1, 135.6, 127.0, 122.8, 121.4, 119.5, 118.5, 118.2, 114.2, 113.0, 112.5, 111.0, 55.7 (OCH₃), 55.7 (OCH₃), 43.5, 27.6; HREI-MS: m/z 438.0233; $[(M+1)^+]$ Calcd for $C_{18}H_{19}BrN_2O_4S$ 438.0248].

2.1.16. *N*-(2-(1*H*-indol-3-yl)ethyl)-2-chloro-5-fluorobenzenesulfonamide (16)

1H NMR (400 MHz DMSO- d_6): δ 13.41 (s, 1H, NH), 10.83 (s, 1H, NH), 7.58 (d, J = 6.5 Hz, 1H), 7.34 (d, J = 6.7 Hz, 1H), 7.27 (dd, J = 7.3, 2.4 Hz, 1H), 7.18–7.14 (m, 2H), 7.07 (t, J = 6.0 Hz, 1H), 6.98 (t, J = 6.2 Hz, 1H), 6.88 (dd, J = 6.0, 6.2 Hz, 1H), 3.90 (t, J = 5.8 Hz, 2H), 3.08 (t, J = 5.8 Hz, 2H); ^{13}C NMR (100 MHz, DMSO- d_6): 167.1 (d, J = 174, C-F), 136.1, 135.0, 132.7, 130.0, 127.0, 122.8, 121.4, 119.5, 118.5, 117.4, 113.5, 112.5, 111.0, 43.5, 27.6; HREI-MS: m/z 352.0436; $[(M+1)^+]$ Calcd for $C_{16}H_{14}ClFN_2O_2S$ 352.0448.

2.1.17. *N*-(2-(1*H*-indol-3-yl)ethyl)-3-bromobenzenesulfonamide (17)

1H NMR (400 MHz DMSO- d_6): δ 12.23 (s, 1H, NH), 11.73 (s, 1H, NH), 7.53 (t, J = 6.3 Hz, 2H), 7.41 (d, J = 6.3 Hz, 1H), 7.30 (d, J = 6.5 Hz, 1H), 7.07 (t, J = 7.5 Hz, 1H), 6.99 (t, J = 6.3 Hz, 1H), 6.94 (t, J = 6.4 Hz, 1H), 6.83 (t, J = 6.6 Hz, 2H), 3.85 (t, J = 4.6 Hz, 5H), 3.09 (t, J = 6.3 Hz, 2H); ^{13}C NMR (100 MHz, DMSO- d_6): δ 142.0, 136.1, 134.5, 130.0, 129.3, 127.0, 126.1, 123.2, 22.8, 121.4, 119.5, 118.5, 112.5, 111.0, 43.5, 27.6; HREI-MS: m/z 378.0023; $[(M+1)^+]$ Calcd for $C_{16}H_{15}BrN_2O_2S$ 378.0037].

2.2. Molecular docking protocol

Molecular docking was performed on the active compounds to identify possible binding modes that explained the reason for their potency. The method used for molecular docking was as mentioned in our previous paper with slight modifications [45]. The molecular docking study was conducted using a homology model for α -glucosidase. The structures of all compounds were prepared using Chem3D by CambridgeSoft. The geometry and energy of the structures were optimized using MMFF94. GOLD was used to identify the binding modes of the active compounds responsible for the activity. The Chemscore fitness function with default settings was employed in this study. The protein sequence for Baker's yeast α -glucosidase (MAL12) was obtained from uniprot (<http://www.uniprot.org>). A homology model for *Saccharomyces cerevisiae* glucosidase was built using the crystal structure of α -D-glucose-bound isomaltase from *S. cerevisiae* (PDB ID: 3A4A), which shares a 72% identical and 85% similar sequence to α -glucosidase. The sequence alignment and homology modeling were performed using Swiss-Model, which is a fully automated homology modeling pipeline (SWISS-MODEL) managed by the Swiss Institute of Bioinformatics. The docking results were visualized using Discovery Studio visualizer 3.5 and PyMol. The homology model was evaluated using PROCHECK.

2.3. α -Glucosidase assay

α -Glucosidase inhibitory activities was determined as per reported methods [46]. 10 μ L of test samples (5 mg/mL DMSO solution) were altered in 100 μ L of 100 mM-phosphate buffer (pH 6.8) in 96-well microplate and incubated with 50 μ L of crude intestinal α -glucosidase for 5 min before 50 μ L substrate (5 mM, *p*-nitrophenyl- α -D-glucopyranoside prepared in same buffer) was added. Release of *p*-nitrophenol

was measured at 405 nm spectrophotometrically (SpectraMax® plus384) for 5 min after incubation with substrate. Individual blanks for test samples were prepared to correct background absorbance where substrate was replaced with 50 μ L of buffer. Control sample contained 10 μ L DMSO in place of test samples. Percentage of enzyme inhibition was calculated as $(1-B/A) \times 100$ where A represents absorbance of control without test samples, and B represents absorbance in presence of test samples. Data found was used for the calculation of IC₅₀ values (concentration at which there is 50% enzyme inhibition)

Enzyme unit Definition: The amount of enzyme required to release one μ mole of glucose per minute from maltose (10 mg/mL) in sodium acetate buffer (100 mM), pH 4.5 at 40 °C.

2.4. In vivo antidiabetic study

Albino Wistar rats were obtained from IRMC animal house. The animals were fed standard diet along with water. The experiments were carried out as per IAU guidelines of Animal Care and Use applicable to animal study and the study was approved by the ethical committee (Ethics Review ID: IRB-2021-300).

2.4.1. Acute oral toxicity study

Synthesized Scaffold 16 was administered to Wistar rats at a dose of 1000 mg/kg body weight to observe the toxicity or lethality of the compound.

2.4.2. STZ induced diabetes

For the present study, albino male wistar rats weighing 170–220 gm were used. To induce the diabetes, 16 h fasted rats were injected intraperitoneally 60 mg/kg Streptozotocin (MOLECULE-ON CAS number 18883-66-4) dissolved in cold citrate buffer of pH 4.5. After injecting the STZ, to prevent the hypoglycaemia, 5% glucose solution will be given per oral for a period of two days. After 5 days of injection, blood glucose level was measured by using glucometer (Accu-chek, Roche), rats with blood glucose level above 200 mg/dL were considered as diabetics and used in the experiments. Animals could access normal food and water during entire study, except prior to the collection of blood sample (fasted blood glucose was measured) [47–49].

2.4.3. Hypoglycemic study

Since there was no information on effective dose of synthesized Scaffold 16 and the compound was found to be safe at a dose of 1000 mg/kg, hence we have selected scalar doses 10, 25, and 50 mg/kg body weight. The effect of these Scaffold doses on fasting blood glucose levels was determined by administering orally and blood glucose level was measured by using glucometer (Accu-chek, Roche) at the interval of 0, 0.5, 1, 2, 4 and 6 h following treatment by tail vein method under mild sevoflurane anaesthesia [47–49]. Each group was consisting of 6 animals ($n = 6$).

2.4.4. Effects of Scaffold-16 on blood glucose and body weight

The animals were grouped as follows and each group was consisting of 6 animals ($n = 6$):

- Group 1: Normal control; Received water
- Group 2: Diabetic Control; Received water
- Group 3: Standard treatment; Received Glibenclamide (5 mg/kg body weight)
- Group 4: Treatment group; Received 25 mg/kg of Scaffold 16
- Group 5: Treatment group; Received 50 mg/kg of Scaffold 16

Fasting blood glucose levels and body weights were measured at 1st, 7th, 14th, 21st and 28th day of the study.

2.4.5. Oral glucose tolerance test (OGTT) in Streptozotocin-induced diabetic rats

OGTT was carried on 28th day of the study. The animals were divided and grouped as: Diabetic control, Standard treatment group, Scaffold 16 (25 and 50 mg/kg body weight). The diabetic control and standard group of animals received normal saline and Glibenclamide 5 mg/kg body weight, respectively. The group 3 and 4 received Scaffold 16 at the dose of 25 mg and 50 mg/kg, per oral. After overnight fasting, a baseline ($t = 0$ h) blood sample was taken from rats of respective groups and 2 g/kg p.o. of Glucose was fed 0.5 h after Scaffold 16 (oral) administration. Blood glucose levels was measured at the interval of 0, 0.5, 1, and 2 h following treatment by tail vein method under mild sevoflurane anaesthesia [47–49].

2.4.6. Statistical analysis

Statistical analysis was performed using analysis of variance (ANOVA) followed by Tukey's post-hoc test through GraphPad Prism v8.02 (GraphPad Software Inc.,). $p < 0.05$ was considered to indicate a statistically significant difference between values.

3. Conclusions

New hybrid class of indole bearing sulfonamide scaffolds (1–17) as α -glucosidase inhibitors were synthesized. All scaffolds exhibited excellent to good potency with IC_{50} values ranging from 1.60 ± 0.010 to $51.20 \pm 1.10 \mu M$ in comparison with standard acarbose ($IC_{50} = 42.45 \pm 1.05 \mu M$) except scaffold 17 which was inactive. Among the synthesized hybrid class scaffolds 1 was the most potent analogue with IC_{50} value $1.60 \pm 0.010 \mu M$, showing ~26-fold better potency as compare to standard acarbose. Scaffolds 1–15 showed an excellent α -glucosidase inhibitory potency as compared to standard. Scaffold 16 showed excellent potency with IC_{50} value $1.60 \mu M$, as compared to standard (42.45 ± 1.05). Antidiabetic potential of Scaffold 16 was further confirmed in STZ induced diabetic rat model. Among the synthesized class, scaffold 17 was found inactive. All analogues were characterized through 1H , ^{13}C NMR and HREI-MS analysis. Structure activity relationship of synthesized new hybrid class were established and confirmed through molecular docking study.

Declaration of Competing Interest

The authors declare that they have no known competing financial interests or personal relationships that could have appeared to influence the work reported in this paper.

Acknowledgements

Authors are thankful to Institute for Research and Medical Consultations (IRMC), Imam Abdulrahman Bin Faisal University for providing excellent research facilities. Further would like to acknowledge Malaysian Ministry of Higher Education (KPT) for the financial support under FRGS Grant File No. 600-IRMI/ FRGS 5/3 (111/2019).

Appendix A. Supplementary material

Supplementary data to this article can be found online at <https://doi.org/10.1016/j.bioorg.2021.104808>.

References

- [1] P. Taslimi, İ. Gülçin, Antidiabetic potential: in vitro inhibition effects of some natural phenolic compounds on α -glucosidase and α -amylase enzymes, *J. Biochem. Mol. Toxicol.* 10 (2017) 21956.
- [2] F. Erdemir, D.B. Celepci, A. Aktaş, P. Taslimi, Y. Gök, H. Karabıyık, İ. Gülçin, 2-Hydroxyethyl substituted NHC precursors: synthesis, characterization, crystal structure and carbonic anhydrase, α -glucosidase, butyrylcholinesterase, and acetylcholinesterase inhibitory properties, *J. Mol. Struct.* 1155 (2018) 797–806.
- [3] İ. Gülçin, P. Taslimi, A. Aygün, N. Sadeghian, E. Bastem, O.I. Kufrevioglu, F. Turkan, F. Şen, Antidiabetic and antiparasitic potentials: inhibition effects of some natural antioxidant compounds on α -glucosidase, α -amylase and human glutathione S-transferase enzymes, *Int. J. Biol. Macromol.* 119 (2018) 741–746.
- [4] J. Yang, X. Wang, C. Zhang, L. Ma, T. Wei, Y. Zhao, X. Peng, Comparative study of inhibition mechanisms of structurally different flavonoid compounds on α -glucosidase and synergistic effect with acarbose, *Food Chem.* 347 (2021), 129056.
- [5] M.Y. Kim, S.W. Choi, Can Walnut serve as a magic bullet for the management of non-alcoholic fatty liver disease? *Appl. Sci.* 11 (2021) 218.
- [6] F. Saleem, K.M. Khan, S. Chigurupati, M. Solangi, A.R. Nemala, M. Mushtaq, Z. Ul-Haq, M. Taha, S. Perveen, Synthesis of azachalcones, their α -amylase, α -glucosidase inhibitory activities, kinetics, and molecular docking studies, *Bioorg. Chem.* 106 (2021), 104489.
- [7] V. Krishnan, R. Rani, M. Awana, D. Pitale, A. Kulshreshtha, S. Sharma, H. Bollinedi, A. Singh, B. Singh, A.K. Singh, S. Praveen, Role of nutraceutical starch and proanthocyanidins of pigmented rice in regulating hyperglycemia: enzyme inhibition, enhanced glucose uptake and hepatic glucose homeostasis using in vitro model, *Food Chem.* 335 (2021), 127505.
- [8] T. Iijima, K. Aoki, Y. Kondo, Y. Terauchi, Comparison of lipid-lowering effects of anagliptin and miglitol in patients with type 2 diabetes: a randomized trial, *J. Clin. Med. Res.* 12 (2020) 73.
- [9] E.O. Ayua, S.G. Nkhata, S.J. Namaumbo, E.H. Kamau, T.N. Ngoma, K.O. Aduol, Polyphenolic inhibition of enterocytic starch digestion enzymes and glucose transporters for managing type 2 diabetes may be reduced in food systems, *Heliyon* 7 (2021) 6245.
- [10] M. Zengin, H. Genc, P. Taslimi, A. Kestane, E. Guclu, A. Ogutlu, O. Karabay, I. Gulcin, Novel thymol bearing oxypropanolamine derivatives as potent some metabolic enzyme inhibitors—Their antidiabetic, anticholinergic and antibacterial potentials, *Bioorg. Chem.* 81 (2018) 119–126.
- [11] A. Bicer, P. Taslimi, G. Yakali, I. Gülçin, M.S. Gültekin, G.T. Cin, Synthesis, characterization, crystal structure of novel bis-thiomethylcyclohexanone derivatives and their inhibitory properties against some metabolic enzymes, *Bioorg. Chem.* 82 (2019) 393–404.
- [12] C. Bayrak, P. Taslimi, H.S. Karaman, I. Gulcin, A. Menzek, The first synthesis, carbonic anhydrase inhibition and anticholinergic activities of some bromophenol derivatives with S including natural products, *Bioorg. Chem.* 85 (2019) 128–139.
- [13] O. Talaz, I. Gülçin, S. Göksu, N. Saracoglu, Antioxidant activity of 5, 10-dihydroindeno [1, 2-b] indoles containing substituents on dihydroindeno part, *Bioorg. Med. Chem.* 17 (2009) 6583–6589.
- [14] U.M. Kocuyigit, Y. Budak, M.B. Gürdere, Ş. Tekin, T.K. Köprülü, F. Ertürk, K. Özcan, İ. Gülçin, M. Ceylan, Synthesis, characterization, anticancer, antimicrobial and carbonic anhydrase inhibition profiles of novel (3aR, 4S, 7R, 7aS)-2-(4-(E)-3-(3-aryl) acryloyl) phenyl)-3a, 4, 7, 7a-tetrahydro-1H-4, 7-methanoisindole-1, 3 (2H)-dione derivatives, *Bioorg. Chem.* 70 (2017) 118–125.
- [15] H. Hussain, M. Nazir, M. Saleem, A. Al-Harasi, I.R. Green, Fruitful decade of fungal metabolites as anti-diabetic agents from 2010 to 2019: emphasis on α -glucosidase inhibitors, *Phytochem. Rev.* 1–35 (2021) (2021).
- [16] R. Rafique, K.M. Khan, S. Chigurupati, A. Wadood, A.U. Rehman, U. Salar, V. Venugopal, S. Shamim, M. Taha, S. Perveen, Synthesis, in vitro α -amylase inhibitory, and radicals (DPPH & ABTS) scavenging potentials of new N-sulfonohydrazide substituted indazoles, *Bioorg. Chem.* 94 (2020), 103410.
- [17] M. Alomari, M. Taha, F. Rahim, M. Selvaraj, N. Iqbal, S. Chigurupati, S. Hussain, N. Uddin, N.B. Almandil, M. Nawaz, R.K. Farooq, Synthesis of indole-based-thiadiazole derivatives as a potent inhibitor of α -glucosidase enzyme along with in silico study, *Bioorg. Chem.* 108 (2021), 104638.
- [18] R. Tundis, M.R. Loizzo, F. Menichini, Natural products as α -amylase and α -glucosidase inhibitors and their hypoglycaemic potential in the treatment of diabetes: an update, *Mini Rev. Med. Chem.* 10 (2010) 315–331.
- [19] P. Li, M. Zhang, H. Li, R. Wang, H. Hou, X. Li, K. Liu, H. Chen, New prenylated indole homodimeric and pteridine alkaloids from the marine-derived fungus *Aspergillus austroafricanus* Y32–2, *Marine Drugs* 19 (2021) 98.
- [20] N. Bhardwaj, A. Pathania, P. Kumar, Naturally available nitrogen-containing fused heterocyclics as prospective lead molecules in medicinal chemistry, *Curr. Trad. Med.* 7 (2021) 5–27.
- [21] T. Meng, Y. Hou, C. Shang, J. Zhang, B. Zhang, Recent advances in indole dimers and hybrids with antibacterial activity against methicillin-resistant *Staphylococcus aureus*, *Archiv der Pharmazie* 354 (2021) 2000266.
- [22] Y. Chen, L. Zhang, L. Zhang, Q. Jiang, L. Zhang, Discovery of indole-3-butyric acid derivatives as potent histone deacetylase inhibitors, *J. Enzyme Inhib. Med. Chem.* 36 (2021) 425–436.
- [23] S. Imran, M. Taha, N.H. Ismail, A review of bisindolylmethane as an important scaffold for drug discovery, *Cur. Med Chem.* 22 (2015) 4412–4433.
- [24] T. Takahashi, H. Inoue, M. Horigome, K. Momose, M. Sugita, K. Katsuyama, C. Suzuki, S. Nagai, M. Nagase, K. Nakamaru, Nissin Seifun Group Inc, Indole derivatives and anti-ulcer compositions thereof. U.S. Patent No. 5, 252, 580, U.S. Patent and Trademark Office, Washington, DC, 1993.
- [25] J.C. Delorenzi, M. Attias, C.R. Gattass, M. Andrade, C. Rezende, A. da Cunha Pinto, A.T. Henriques, D.C. Bou-Habib, E.M. Saraiva, Antileishmanial activity of an indole alkaloid *Frompesciera australis*, *Antimicrob. Agents Chemother.* 45 (2001) 1349–1354.
- [26] M.K. Park, Y.H. Rhee, H.J. Lee, E.O. Lee, K.H. Kim, M.J. Park, B.H. Jeon, B.S. Shim, C.H. Jung, S.H. Choi, K.S. Ahn, Antiplatelet and antithrombotic activity of indole-3-carbinol in vitro and in vivo, *Phytother. Res.* 22 (2008) 58–64.

- [27] W. Hui, Y. Dai, Therapeutic potential of aryl hydrocarbon receptor ligands derived from natural products in rheumatoid arthritis, *Basic Clin. Pharmacol. Toxicol.* 126 (2020) 469–474.
- [28] S. Stüzen, Antioxidant activities of synthetic indole derivatives and possible activity mechanisms, *Bioactive Heterocycles V* (2007) 145–178.
- [29] D. Yu, M. Suzuki, L. Xie, S.L. Morris-Natschke, K.H. Lee, Recent progress in the development of coumarin derivatives as potent anti-HIV agents, *Med. Res. Rev.* 23 (2003) 322–345.
- [30] M. Taha, E.A.J. Aldhamin, N.B. Almandil, N. Uddin, M. Alomari, F. Rahim, B. Adalat, M. Ibrahim, F. Nawaz, N. Iqbal, B. Alghanem, Synthesis of indole based acetohydrazide analogs: their in vitro and in silico thymidine phosphorylase studies, *Bioorg. Chem.* 98 (2020), 103745.
- [31] N.B. Almandil, M. Taha, M. Gollapalli, F. Rahim, M. Ibrahim, A. Mosaddik, Indole bearing thiadiazole analogs: synthesis, β -glucuronidase inhibition and molecular docking study, *BMC Chem.* 13 (2019) 1–10.
- [32] H. Azevedo-Barbosa, D.F. Dias, L.L. Franco, J.A. Hawkes, D.T. Carvalho, From antibacterial to antitumour agents: a brief review on the chemical and medicinal aspects of sulfonamides, *Mini Rev. Med. Chem.* 20 (2020) 2052–2066.
- [33] S.R. Wegst-Uhrich, D.A. Navarro, L. Zimmerman, D.S. Aga, Assessing antibiotic sorption in soil: a literature review and new case studies on sulfonamides and macrolides, *Chem. Cent. J.* 8 (2014) 1–12.
- [34] U. Kosak, B. Brus, D. Knez, S. Zakelj, J. Trontelj, A. Pisljar, R. Sink, M. Jukić, M. Zivin, A. Podkova, F. Nachon, The magic of crystal structure-based inhibitor optimization: development of a butyrylcholinesterase inhibitor with picomolar affinity and in vivo activity, *J. Med. Chem.* 61 (2018) 119–139.
- [35] U. Kosak, B. Brus, D. Knez, R. Sink, S. Zakelj, J. Trontelj, A. Pisljar, J. Šlenc, M. Gobec, M. Zivin, L. Tratnjek, Development of an in-vivo active reversible butyrylcholinesterase inhibitor, *Sci. Rep.* 6 (2016) 1–16.
- [36] S. Riaz, I.U. Khan, M. Bajda, M. Ashraf, A. Shaikat, T.U. Rehman, S. Mutahir, S. Hussain, G. Mustafa, M. Yar, Pyridine sulfonamide as a small key organic molecule for the potential treatment of type-II diabetes mellitus and alzheimer's disease. In vitro studies against yeast α -glucosidase, acetylcholinesterase and butyrylcholinesterase, *Bioorg. Chem.* 63 (2015) 64–71.
- [37] P. Zajdel, A. Partyka, K. Marciniak, A.J. Bojarski, M. Pawlowski, A. Wesolowska, Quinoline- and isoquinoline-sulfonamide analogs of aripiprazole: novel antipsychotic agents, *Future Med. Chem.* 6 (2014) 57–75.
- [38] S. Mutahir, J. Jończyk, M. Bajda, I.U. Khan, M.A. Khan, N. Ullah, M. Ashraf, S. Riaz, S. Hussain, M. Yar, Novel biphenyl bis -sulfonamides as acetyl and butyrylcholinesterase inhibitors: synthesis, biological evaluation, and molecular modeling studies, *Bioorg. Chem.* 64 (2016) 13–20.
- [39] M. Morris, G.M. Knudsen, S. Maeda, J.C. Trinidad, A. Ioanoviciu, A.L. Burlingame, L. Mucke, Tau post-translational modifications in wild-type and human amyloid precursor protein transgenic mice, *Nat. Neurosci.* 18 (2015) 1183–1189.
- [40] H.I. Gul, C. Yamali, H. Sakagami, A. Angeli, J. Leitans, A. Kazaks, K. Tars, D. O. Ozgun, C.T. Supuran, New anticancer drug candidates' sulfonamides as selective hCA IX or hCA XII inhibitors, *Bioorg. Chem.* 77 (2018) 411–419.
- [41] a) M. Taha, S.A.A. Shah, M. Afifi, S. Imran, S. Sultan, F. Rahim, K.M. Khan, Synthesis, α -glucosidase inhibition, and molecular docking study of coumarin based derivatives, *Bioorg. Chem.* 77 (2018) 586–592. b) M. Taha, S.A.A. Shah, M. Afifi, S. Imran, S. Sultan, F. Rahim, N.H. Ismail, K.M. Khan, Synthesis, molecular docking study and thymidine phosphorylase inhibitory activity of 3-formylcoumarin derivatives, *Bioorg. Chem.* 78 (2018) 17–23. c) H. Ullah, F. Rahim, M. Taha, I. Uddin, A. Wadood, S.A.A. Shah, R.K. Farooq, M. Nawaz, Z. Wahab, K.M. Khan, Synthesis, molecular docking study and in vitro thymidine phosphorylase inhibitory potential of oxadiazole derivatives, *Bioorg. Chem.* 78 (2018) 58–67. d) M. Aha, M.S. Baharudin, N.H. Ismail, S. Imran, M.N. Khan, F. Rahim, M. Selvaraj, S. Chigurupati, M. Nawaz, F. Qureshi, S. Vijayabalan, Synthesis, α -amylase inhibitory potential and molecular docking study of indole derivatives, *Bioorg. Chem.* 80 (2018) 36–42. e) T. Noreen, M. Taha, S. Imran, S. Chigurupati, F. Rahim, M. Selvaraj, N.H. Ismail, J.I. Mohammad, H. Ullah, F. Nawaz, M. Irshad, Synthesis of alpha amylase inhibitors based on privileged indole scaffold, *Bioorg. Chem.* 72 (2017) 248–255. f) M. Taha, S. Imran, N.H. Ismail, M. Selvaraj, F. Rahim, S. Chigurupati, H. Ullah, F. Khan, U. Salar, M.T. Javid, S. Vijayabalan, Biology-oriented drug synthesis (BIODS) of 2-(2-methyl-5-nitro-1H-imidazol-1-yl) ethyl aryl ether derivatives, in vitro α -amylase inhibitory activity and in silico studies, *Bioorg. Chem.* 74 (2017) 1–9. g) M. Taha, F. Rahim, S. Imran, N.H. Ismail, H. Ullah, M. Selvaraj, M.T. Javid, U. Salar, M. Ali, K.M. Khan, Synthesis, α -glucosidase inhibitory activity and in silico study of tris-indole hybrid scaffold with oxadiazole ring: as potential leads for the management of type-II diabetes mellitus, *Bioorg. Chem.* 74 (2017) 30–40. h) M. Taha, M.T. Javid, S. Imran, M. Selvaraj, S. Chigurupati, H. Ullah, F. Rahim, F. Khan, J.I. Mohammad, K.M. Khan, Synthesis and study of the α -amylase inhibitory potential of thiadiazole quinoline derivatives, *Bioorg. Chem.* 74 (2017) 179–186. i) M. Taha, S. Imran, F. Rahim, A. Wadood, K.M. Khan, Oxindole based oxadiazole hybrid analogs: novel α -glucosidase inhibitors, *Bioorg. Chem.* 76 (2018) 273–280.
- [42] N. Öztaşkın, R. Kaya, A. Maraş, E. Şahin, İ. Gülcin, S. Göksu, Synthesis and characterization of novel bromophenols: determination of their anticholinergic, antidiabetic and antioxidant activities, *Bioorg. Chem.* 87 (2019) 91–102.
- [43] H.G. Bilgili, A. Kestane, P. Taslimi, O. Karabay, A. Bytyqi-Damoni, M. Zengin, I. Gulcin, Novel eugenol bearing oxypropanolamines: synthesis, characterization, antibacterial, antidiabetic, and anticholinergic potentials, *Bioorg. Chem.* 88 (2019), 102931.
- [44] F. Erdemir, D.B. Celepci, A. Aktaş, Y. Gök, R. Kaya, P. Taslimi, Y. Demir, I. Gulcin, Novel 2-aminopyridine liganded Pd (II) N-heterocyclic carbene complexes: Synthesis, characterization, crystal structure and bioactivity properties, *Bioorg. Chem.* 91 (2019), 103134.
- [45] S. Imran, M. Taha, N.H. Ismail, S.M. Kashif, F. Rahim, W. Jamil, M. Hariono, M. Yusuf, H. Wahab, Synthesis of novel flavone hydrazones: in-vitro evaluation of α -glucosidase inhibition, QSAR analysis and docking studies, *Eur. J. Med. Chem.* 105 (2015) 156–170.
- [46] L.R. Guerreiro, E.P. Carreiro, L. Fernandes, T.A. Cardote, R. Moreira, A.T. Caldeira, R.C. Guedes, A.J. Burke, Five-membered iminocyclitol α -glucosidase inhibitors: synthetic, biological screening and in silico studies, *Bioorg. Med. Chem.* 21 (2013) 1911–1917.
- [47] M.D. Salahuddin, S.S. Jalalpure, N.B. Gadge, Antidiabetic activity of aqueous bark extract *Cassia glauca* in streptozotocin-induced diabetic rats, *Canadian J. Physiol. Pharmacol.* 88 (2010) 153–160.
- [48] Y. Nayak, V. Hillemane, V.K. Daroji, B.S. Jayashree, M.K. Unnikrishnan, Antidiabetic activity of benzopyrone analogues in nicotinamide-streptozotocin induced type 2 diabetes in rats, *Sci. World J.* 12 (2014) 85426.
- [49] D.G. Hai, L. Peng, Y. Yang, G. Fang, Sulfonamide-1,3,5-triazine-thiazoles: discovery of a novel class of antidiabetic agents via inhibition of DPP-4, *RSC Adv.* 6 (2016) 83438–83447.